Irradiation and testbeam of KEK/HPK planar p-type pixel modules for HL-LHC

2015 JINST 10 C06008

(http://iopscience.iop.org/1748-0221/10/06/C06008)

PUBLISHED BY IOP PUBLISHING FOR SISSA MEDIALAB

RECEIVED: *January 16, 2015*
ACCEPTED: *April 16, 2015*
PUBLISHED: *June 16, 2015*

PIXEL 2014 INTERNATIONAL WORKSHOP
SEPTEMBER 1–5, 2014
NIAGARA FALLS, CANADA

2015 JINST 10 C06008

Irradiation and testbeam of KEK/HPK planar p-type pixel modules for HL-LHC

K. Nakamura,[a,1] **Y. Arai,**[b] **M. Hagihara,**[c] **K. Hanagaki,**[b] **K. Hara,**[c] **R. Hori,**[a] **M. Hirose,**[d] **Y. Ikegami,**[a] **O. Jinnouchi,**[d] **S. Kamada,**[e] **K. Kawagoe,**[f] **T. Kohno,**[g] **K. Motohashi,**[d] **R. Nishimura,**[h] **S. Oda,**[f] **H. Otono,**[f] **Y. Takubo,**[a] **S. Terada,**[a] **R. Takashima,**[h] **J. Tojo,**[f] **Y. Unno,**[a] **J. Usui,**[c] **T. Wakui,**[i] **D. Yamaguchi,**[d] **K. Yamamoto**[h] **and K. Yamamura**[e]

[a] *High Energy Accelerator Research Organization, Oho 1-1, Tsukuba-shi, Ibaraki-ken, Japan*
[b] *Department of Physics, Osaka Univeristy, Toyonaka, Osaka 56, Japan*
[c] *Institute of Pure and Applied Sciences, Univeristy of Tsukuba, Tennodai 1-1, Tsukuba-shi, Ibaraki-ken, Japan*
[d] *Department of Physics, Tokyo Institute of Technology, 2-12-1 Oh-okayama, Meguro, Tokyo, Japan*
[e] *Hamamatsu Photonics K.K., Hamamatsu, 435, Japan*
[f] *Experimental Particle Physics, Kyushu University, Hakosaki 6-10-1, Higashi-ku, Fukuoka-shi, Fukuoka-ken, Japan*
[g] *Department of Physics, Ochanomizu University, 1-1 Otsuka 2, Bunkyo-ku, Tokyo, Japan*
[h] *Department of Physics, Kyoto University of Education, Kyoto, Japan*
[i] *Cyclotron and Radioisotope Center, Tohoku University, 6-3 Aoba, Aramaki, Aoba-ku, Sendai, Miyagi 980-8578, Japan*

E-mail: Koji.Nakamura@cern.ch

[1] Corresponding author.

doi:10.1088/1748-0221/10/06/C06008

ABSTRACT: For the ATLAS detector upgrade for the high luminosity LHC (HL-LHC), an n-in-p planar pixel sensor-module is being developed with HPK. The modules were irradiated at the Cyclotron RadioIsotope Center (CYRIC) using 70 MeV protons. For the irradiation, a novel irradiation box has been designed that carries 16 movable slots to irradiate the samples slot-by-slot independently, to reduce the time for replacing the samples by hand, thus reducing the irradiation to human body. The box can be moved horizontally and vertically to scan the samples for a maximum area of 11 cm x 11 cm. Tests were subsequently carried out with beam at CERN by using 120 GeV pions and at DESY with 4 GeV electrons. We describe the analyses of the testbeam data of the KEK/HPK sensor-modules, focussing on the comparison of the performance of old and new designs of pixel structures, together with a reference of the simplest design (no biasing structure). The novel design has shown comparably good performance as the no-structure design in detecting passing-through charged particles.

KEYWORDS: Radiation damage to electronic components; Radiation damage evaluation methods; Radiation damage to detector materials (solid state); Large detector systems for particle and astroparticle physics

2015 JINST 10 C06008

Contents

1 Introduction **1**
- 1.1 High Luminosity LHC and ATLAS upgrade 1
- 1.2 Planar pixel sensor detector 2
- 1.3 New sensor structure 3

2 Irradiation test **4**
- 2.1 Irradiation facility at CYRIC 4
- 2.2 Irradiation setup 4
- 2.3 Fluence calculation 5

3 Testbeam **6**
- 3.1 Testbeam setup and analysis 6
- 3.2 Results 6

4 Conclusion **7**

2015 JINST 10 C06008

1 Introduction

The physics experiment programme at the Large Hadron Collider (LHC) [1] operated successfully for three years (2010-2012). The observation of a Higgs boson with a mass of approximately 125 GeV by the ATLAS [2] and CMS Collaborations [3, 4] was an important milestone. Further investigation of the origin of electroweak symmetry breaking [5, 6] and the experimental confirmation as well as the search for Beyond the Standard Model (BSM) phenomenology are the primary task for the LHC experiment and its upgrade projects known as the High Luminosity LHC (HL-LHC).

1.1 High Luminosity LHC and ATLAS upgrade

The High Luminosity LHC is a project which relies on new accelerator technology, such as cutting-edge 13 Tesla super conducting magnets, precise superconducting cavities for beam rotation and 300-metre-long high-power superconducting links. Together with the accelerator upgrade enhancements, The upgrade of ATLAS and CMS detectors with further high-speed front end readout for the improved detectors are planed. Main physics motivations of these upgrade projects are observation of small coupling to Higgs Boson such as muon Yukawa coupling, probe of Higgs tri-linear coupling and further BSM searches. After the upgrade of the ATLAS experiment with first physics around 2025, the Inner Tracking Detector (ID) [7] will be designed for 10 years of operation, at a peak instantaneous luminosity of 5×10^{34} cm^{-2}s^{-1}, 14 TeV centre-of-mass energy and 25ns between beam crossing. Since the high instantaneous luminosity introduces about 140 average interaction of protons in a bunch crossing, vertex identification is very important and the ID is the

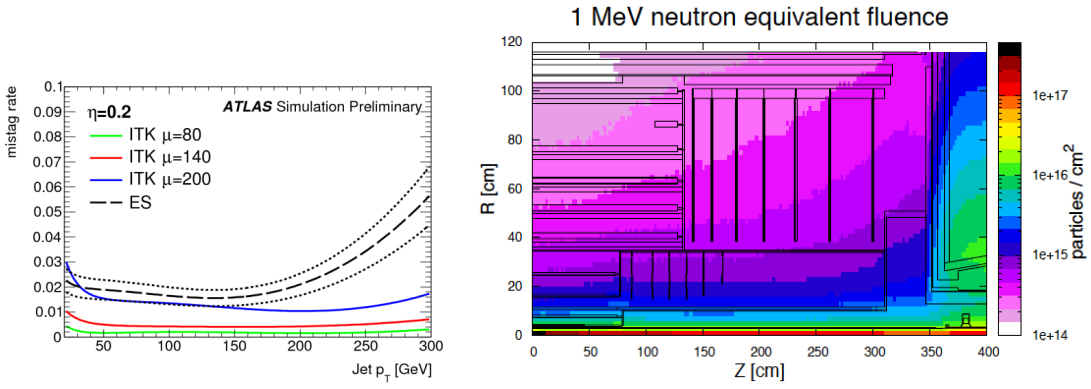

(a) **(b)**

Figure 1. (a) The performance of mis-identification rate for b-tagging as a function of transverse momentum of jets. The green, red and blue lines show the mis-identification rates for the 80, 140 and 200 average interaction per bunch crossing. (b) The fluence map at $\int Ldt = 3000$ fb^{-1} for the typical layout.

key element. As an example, the performance of mis-identification rates for b-tagging while keeping the same identification efficiency for cases of 80, 140 and 200 proton collisions are shown in figure 1a. The mis-identification rate gets worse about a factor of 3-5. Furthermore the radiation environment of the inner detector is extreme. An integrated luminosity $\int Ldt = 3000$ fb^{-1} of data will be accumulated by ATLAS. Figure 1b shows the radiation fluence map at the full integrated luminosity as the unit of the 1 MeV neutron equivalent flux per 1 cm^2 area. The fluence of Inner pixel layer, 3 cm distance from vertex position, and outer layer, 35 cm from vertex position, are around 1.4×10^{16} 1 MeVn$_{\rm eq}$/cm^2 and 1.7×10^{15} 1 MeVn$_{\rm eq}$/cm^2 without any safety factor, respectively. Accordingly, making radiation tolerant pixel detectors which usable during the 10 years high-luminosity operation is one of important goal of this study. To confirm the performance of the radiation tolerability, irradiation tests by proton beam were performed by CYRIC irradiation facility at Tohoku University as well as testbeams by positron and pion beam at CERN and DESY.

1.2 Planar pixel sensor detector

One of major options of radiation tolerant pixel detector for the outer pixel layer is "Planar Pixel Sensor" [8, 9]. The R&D program of KEK develops n-in-p planar pixel sensor and modules manufactured by Hamamatsu Photonix K.K. (HPK) with the ATLAS Japan Silicon Group [10–12]. Figure 2a shows a picture of a KEK developed module which has four modules in a printed circuit board, also know as "4-chip-card". The FE-I4 [13] read-out chips , presently installed in the IBL [14], are put on the sensors connected by SnAg bump bonding. Read-out data includes the information of time-over-threshold (ToT) as 4 bit analog data. Tuning parameters of the chip are set to make 7ToT for the number of electron-hole pairs by a passing-through MIP particle signal. For the threshold to obtain ToT are set about 1800-2600 electron depends on the thickness of the modules.

As results in the testbeam at CERN in 2012 [10], the inefficiency regions are typically at the pixel boundary regions as shown in figure 2b. Top and middle figures show efficiency maps around one pixel for before and after irradiation (fluence is 1.0×10^{16} 1 MeVn$_{\rm eq}$). The efficiency in

2015 JINST 10 C06008

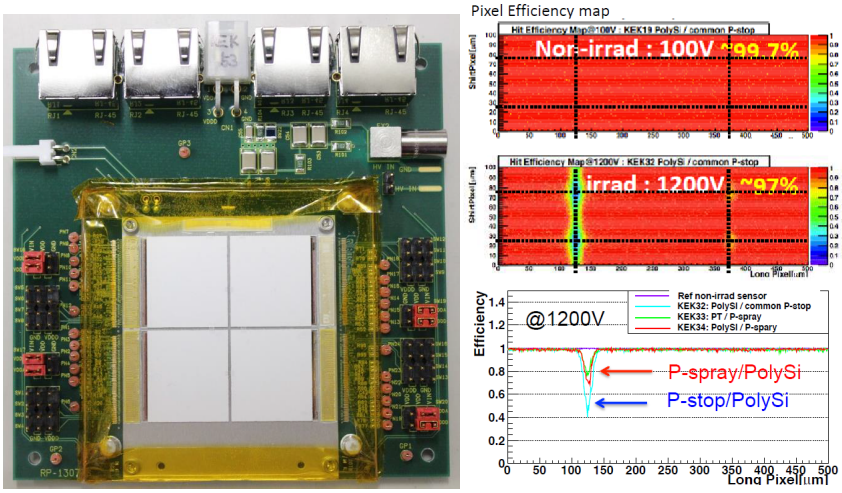

(a) **(b)**

Figure 2. (a) a picture of the KEK developed module which has four modules in a printed circuit board. (b) Illustrating an issue of efficiency drop after irradiation. Top two figures show hit efficiency maps for one pixel with and nearby half-pixels where black dash lines are pixel boundaries. Top and middle maps correspond to before and after proton irradiation. The bottom figure shows a projection of hit efficiency map in the long pixel direction after irradiation. The colors indicate the different sensor structures.

the pixel boundary region drops significantly compared to the center area of the electrode. Figure 2b(bottom) shows a projection of the hit efficiency map in the long pixel direction after irradiation.

1.3 New sensor structure

One hypothesis which makes the issue presented in the previous section happen is as follows. To supply bias voltage to the sensor before attaching the read-out chip on, biasing structures, bias-rail and bias resistor, are necessary. The traditional sensor structure illustrated in figure 3a has a bias-rail on the P-stop by intermediary of the silicon di-oxide layer for only the left side in the figure, which corresponds to the region of efficiency drop. To avoid biasing structure on the P-stop, three types of new sensor structures are developed. Typically the idea is that the bias-rail and bias resistor (made by "poly-si") which is similar voltage level as bias-rail are placed away from pixel boundary region. For Type 10 shown in the figure 3c has bias-rail made by "poly-si" material are which is with offset and the bias resistors are placed inside of electrode. Figure 3b illustrates the slice of Type 10 structure. Conversely, Type 13 have a wider p-stop structure under the bias-rail which is located in the same position but made by "poly-si" material. The Structure of the bias resistor is the same as Type 10. Type 19 without any biasing structures is considered as ideal case. For the no biasing structure case, since the bias voltage is not be able to be supplied before putting read-out chips on by bump bonding, the quality control at sensor level is not possible. This introduce the reduction of the rate which pass the quality control after bump bonding.

2015 JINST 10 C06008

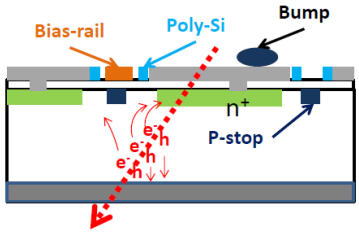

(a) Original structure.

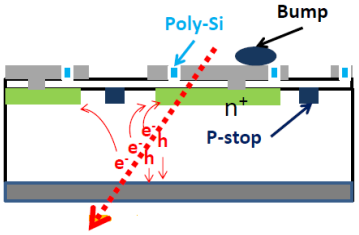

(b) Type 10 structure.

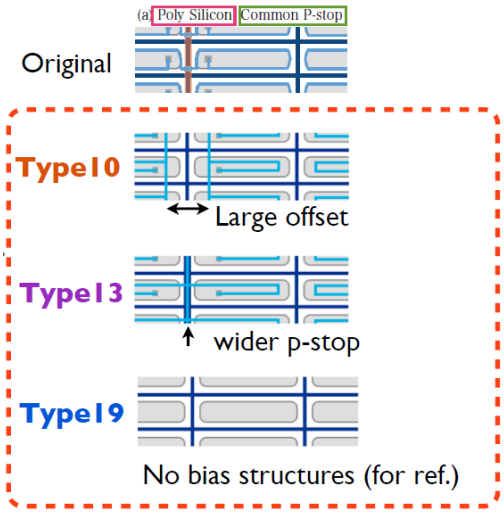

(c) Various sensor structure.

Figure 3. Original and new sensor structures. (a) shows slice of around one pixel region for original sensor. (b) show the same as (a) but new type of sensor. The bias-rail made by "poly-si" material are placed inside of electrode. (c) shows various sensor structure. First and Second shows Original and Type 10 structure correspond to the (a) and (b) respectively. Third shows Type 13 structure which has wider p-stop under the bias-rail. Last shows Type 19 which does not have any "Bias-rail" and bias resistor structures as ideal case.

2 Irradiation test

2.1 Irradiation facility at CYRIC

To qualify the radiation tolerance of the pixel detector, high intensity proton beam is used to irradiate pixel modules. A proton irradiation facility, Cyclotron and Radioisotope Center (CYRIC) at Tohoku University, has an Azimuthal Varying Field (AVF) cyclotron and a beam line for the radiation damage test of semiconductors. The beam line (32 course) supplies the high intensity proton beam with the momentum of 70 MeV and typically 1-1000 nA beam current. The size of beam is tuned to about 5 mmϕ defined as the size of 68% of protons are inside.

2.2 Irradiation setup

Since the high fluence of irradiation makes a risk of high radiation exposure during replacement of modules, an intelligent box is prepared as shown in figure 4a. The box holds 16 layers of support aluminium frame which is used to install silicon modules to be irradiated. Each layer of frames move between two relative positions, target position and evacuated position shown in figure 4b, independently so that irradiation is performed for specific layers and not for the rest. Taking into account the size of target samples, about 40mm $\times$ 40mm of "4-chip-card", as described in section 1.2, the size of beam, about 5mmϕ, is smaller. The intelligent box moved horizontally and vertically to scan the sample and make uniform irradiation for full area of target samples. The scan speed is optimized around 20-50 mm/s due to the number of full area scan required to be at least 20 times during irradiation time. This avoids a non-uniform scan caused by stopping at the

2015 JINST 10 C06008

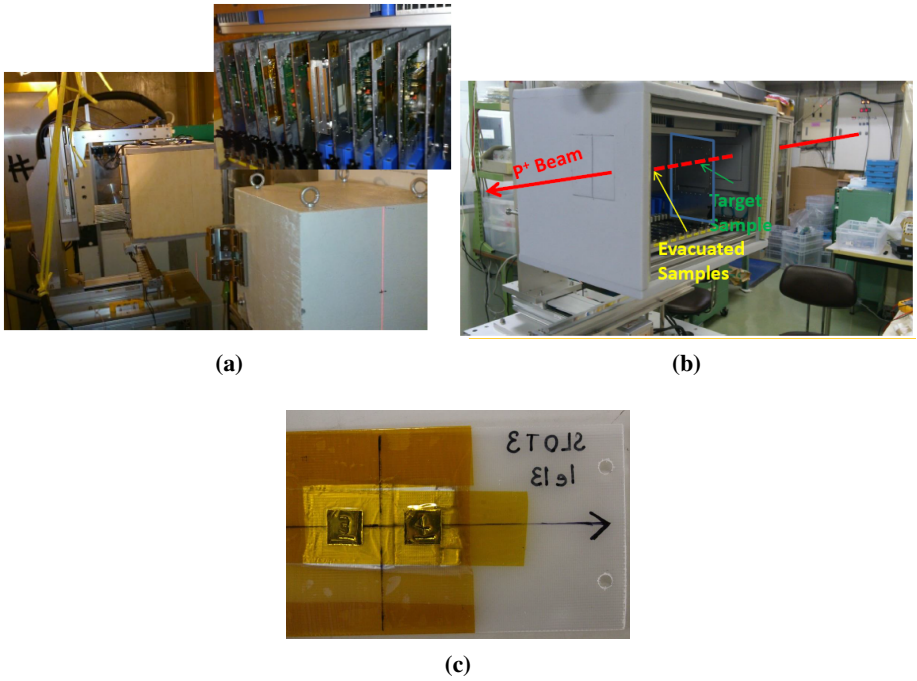

(a) (b)

(c)

Figure 4. A intelligent box for irradiation tests and dosimetry aluminium. (a) A picture of the box installed into the 32 course beam line at CYRIC. The box is on the X-Y stage. The small picture shows the 16 layer of aluminum frame with target modules. (b) illustrating the two positions of aluminum frame, target position and evacuated position. (c) shows irradiation samples. Two aluminum foils with the size of 1 cm×1 cm on the front side are used for the measurement of fluence.

middle of the way of scan (non-uniformity is less than 5%). The energy loss of the 70 MeV proton beam after crossing one layer of "4-chip-card" is approximately 2-3%. The maximum number of modules irradiated at the same time is less than four so that the beam energy keeps over 90% at the front of each module to avoid a difference of cross section and multiple scattering effects.

2.3 Fluence calculation

Measurements of the actual fluence of the irradiation tests are important to confirm target fluence of the irradiation. Fluence is measured using the thin 1 cm^2 size aluminum foil. The nuclear spallation reaction of proton and aluminum, $p + \mathrm{Al} \rightarrow {}^{24}\mathrm{Na} + \mathrm{X}$, produce radioisotope ^{24}Na. The gamma ray from the ^{24}Na is measured by a germanium photon counter. The actual fluence Φ is calculated as follows.

$$\Phi[1\,\mathrm{MeV n_{eq}/cm^2}] = \frac{\mathrm{N_{mes}} e^{\lambda \Delta t}}{\mathrm{N_t}\sigma\lambda\mathrm{E_{eff}}\Gamma} \times 0.7, \tag{2.1}$$

where N_{mes} is the number of γ rays in a second measured by germanium photon counter, λ is the decay constant of ^{24}Na, Δt is time between irradiation and germanium photon counting, N_{t} is the number of aluminum atoms, σ is the ^{24}Na production cross section of nuclear spallation reaction of proton and aluminum, E_{eff} is the efficiency of germanium photon counter and Γ is branching ratio, $\mathrm{BR}(^{24}\mathrm{Na} \rightarrow {}^{24}\mathrm{Mg} + \gamma(1368.6\ \mathrm{keV}))$. The final constant 0.7 at the end is the ratio of Non Ionizing Energy Loss (NIEL) between 1 MeV neutron and 70 MeV proton. The variance of actual fluence

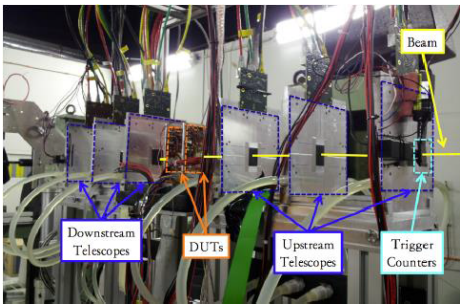

Figure 5. A picture of the testbeam setup. Two set of three telescopes are placed upstream and downstream of DUTs.

value normalized by target fluence for various irradiated samples is about 10% and the dominant uncertainty of absolute fluence is the production cross section (10%). The irradiation of modules are preformed with 600 nA beam current for about 6 hours to make target fluence, $3\times10^{1}5$.

3 Testbeam

Testing the efficiency on the sensor structure needs a precise pointing resolution of the particle passing through. Testbeam by high energy pion or positron beams with high position resolution telescopes are performed. Samples of the original structure were tested in 2012 at CERN as described in [10]. In 2013-2014, new structure samples were tested at DESY.

3.1 Testbeam setup and analysis

Testbeams at CERN and DESY uses 120 GeV π^+ beams and 4 GeV positron beams respectively at an average trigger rate of 500-1000 Hz. Both at CERN and DESY testbeam, the same six layers of EUDET telescope with Minosa 26 sensors [15] are placed at the beam line and device under test (DUT) is installed between third and forth layer as shown in figure 5. The telescope was designed with a less than 3μm pointing resolution at the DUTs without multiple scattering effect. Typical resolution at CERN and DESY are 4.5 μm and 23 μm, respectively. The worse resolution at DESY testbeam than at CERN is caused by multiple scattering effect of 5 GeV positron beam. The ILC Software also know as "Marlin" framework [16, 17] is used for alignment and track reconstruction. The analysis of the reconstructed tracks is conducted in several steps using a dedicated data analysis framework (tbmon) [18].

3.2 Results

The basic performance parameters are measured for irradiated modules with each of three new sensor structures summarized in section 1.3. Overall hit detection efficiency and ToT values of the each modules at a bias voltage of 400 V are summarized in table 1. Overall efficiency is above 99% except for Type 10 modules. Low efficiency of the Type 10 Module is caused by trigger timing issue of data taking and is expected to be roughly close to 100% after correction. Because Telescope read hit data longer time than DUTs, the denominator of the efficiency measurement get larger. This introduce the lower efficiency in the case of only one DUT is installed. ToT values for each sensors are consistent with the tuning target value 7 ToT.

2015 JINST 10 C06008

Table 1. A results of overall Efficiency and ToT for each structure sensors. Low Efficiency of the Type 10 sensor, marked †, compared with the other sample is caused by trigger timing issue of the data taking.

Sensor Type	Sensor Thickness μm	Fluence $_{eq}$/cm^2	Efficiency in percent	ToT value
Type 10	150	4×10^{15}	78.0†	7.0
Type 13	320	3×10^{15}	99.0	8.2
Type 19	150	3×10^{15}	99.5	7.2

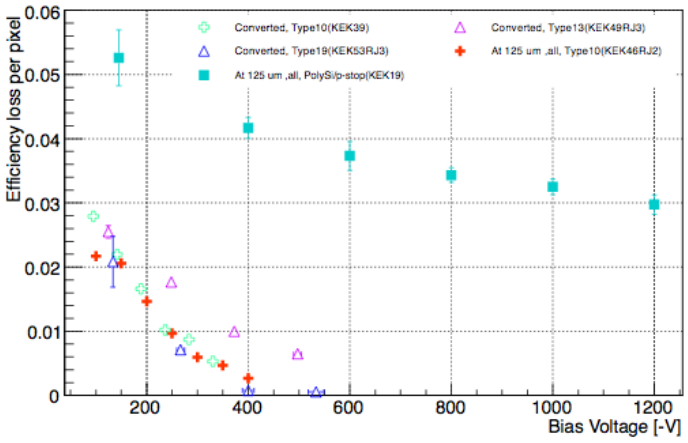

Figure 6. The distributions of ϵ_{loss} as a function of bias voltage for original type (filled square), type 10 (filled and open cross), type 13 (open violet triangle) and type 19 (open blue triangle).

Since efficiency loss is observed at the pixel boundary region as described in section 1.2, projection of efficiency maps are plotted as the same way as shown in figure 2b(bottom). To make quantitative comparison of the efficiency loss, efficiency-loss-per-pixel (ϵ_{loss}) is defined as the efficiency loss of the pixel boundary region. The projection distribution of the efficiency map around biasing structure regions are fitted by constant minus Gaussian function. The distributions of ϵ_{loss} as a function of bias voltage for various type of modules are shown in figure 6. Difference of fluence and thickness are corrected by using a simple shift of the distribution obtained by testbeam data of the different fluence and thickness samples. Large value of ϵ_{loss} indicate large efficiency loss at the pixel boundary region, like the original type of sensor (filled square). The type 19 which there are no biasing structure shows best performance as expected (open blue triangle). Type 10 and Type 13 show as similar ϵ_{loss} distribution as type 19 while type 10 is slightly better performance than type 13.

4 Conclusion

The n-in-p planar type silicon pixel sensors are developed by the ATLAS-Japan Silicon group in the ATLAS Planar Pixel Sensors (PPS) collaboration with HPK. Different types of the sensor structure aiming to improve the efficiency of the pixel boundary regions were examined. Overall efficiency

2015 JINST 10 C06008

over 99% is confirmed with the expected charge detection by ToT after $>3\times10^{15}$ [1 MeVn_{eq}/cm^2] irradiation. The sensor structure with bias-rail made by "poly-si" material are placed with an offset from the pixel boundary and bias resistors which are placed inside of electrodes performed the best out of the tested structures and the performance is almost identical to the ideal case without biasing structures. Further optimization of structure parameters, size of offset for instance, will be tested in the next production.

Acknowledgments

This research was partially supported by a Grant-in-Aid for scientific research on advanced basic research (Grant No. 23104002) from the Ministry of Education, Culture, Sports, Science and Technology, of Japan.

References

[1] *LHC webpage*, http://home.web.cern.ch/about/accelerators/large-hadron-collider; *CERN webpage*, http://home.web.cern.ch.

[2] ATLAS collaboration, G. Aad et al., *The ATLAS experiment at the CERN Large Hadron Collider*, 2008 *JINST* **3** S08003 [INSPIRE].

[3] ATLAS collaboration, G. Aad et al., *Observation of a new particle in the search for the standard model Higgs boson with the ATLAS detector at the LHC*, *Phys. Lett.* **B 716** (2012) 1 [arXiv:1207.7214] [INSPIRE].

[4] CMS collaboration, S. Chatrchyan et al., *Observation of a new boson at a mass of* 125 *GeV with the CMS experiment at the LHC*, *Phys. Lett.* **B 716** (2012) 30 [arXiv:1207.7235] [INSPIRE].

[5] F. Englert and R. Brout, *Broken symmetry and the mass of gauge vector mesons*, *Phys. Rev. Lett.* **13** (1964) 321 [INSPIRE].

[6] P.W. Higgs, *Broken symmetries and the masses of gauge bosons*, *Phys. Rev. Lett.* **13** (1964) 508 [INSPIRE].

[7] ATLAS collaboration, *Letter of intent for the phase-II upgrade of the ATLAS experiment*, CERN-LHCC-2012-022, CERN, Geneva Switzerland (2012) [LHCC-I-023].

[8] J. Weingarten, S. Altenheiner, M. Beimforde, M. Benoit, M. Bomben et al., *Planar pixel sensors for the ATLAS upgrade: beam tests results*, 2012 *JINST* **7** P10028 [arXiv:1204.1266] [INSPIRE].

[9] C. Gallrapp, *Planar pixel sensors for the ATLAS tracker upgrade at HL-LHC*, *Nucl. Instrum. Meth.* **A 718** (2013) 323 [arXiv:1206.3442] [INSPIRE].

[10] K. Motohashi, T. Kubota, K. Nakamura, R. Hori, C. Gallrapp et al., *Evaluation of KEK n-in-p planar pixel sensor structures for very high radiation environments with testbeam*, *Nucl. Instrum. Meth.* **A 765** (2014) 125 [INSPIRE].

[11] Y. Unno, C. Gallrapp, R. Hori, J. Idarraga, S. Mitsui et al., *Development of novel n^+-in-p silicon planar pixel sensors for HL-LHC*, *Nucl. Instrum. Meth.* **A 699** (2013) 72 [INSPIRE].

[12] R. Nagai, J. Idarraga, C. Gallrapp, Y. Unno, A. Lounis et al., *Evaluation of novel KEK/HPK n-in-p pixel sensors for ATLAS upgrade with testbeam*, *Nucl. Instrum. Meth.* **A 699** (2013) 78 [INSPIRE].

2015 JINST 10 C06008

[13] M. Barbero, D. Arutinov, R. Beccherle, G. Darbo, S. Dube et al., *Submission of the first full scale prototype chip for upgraded ATLAS pixel detector at LHC, FE-I4A*, *Nucl. Instrum. Meth.* **A 650** (2011) 111 [INSPIRE].

[14] M. Capeans et al., *ATLAS insertable B-layer technical design report*, CERN-LHCC-2010-013, CERN, Geneva Switzerland (2010) [ATLAS-TDR-019].

[15] EUDET-JRA1 collaboration, A. Bulgheroni, *Results from the EUDET telescope with high resolution planes*, *Nucl. Instrum. Meth.* **A 623** (2010) 399 [INSPIRE].

[16] J. Behr, *Test beam measurements with the EUDET pixel telescope*, EUDET-Report-2010-01, (2010).

[17] D. Cussans, *A trigger/timing logic unit for ILC test-beams*, contribution to *TWEPP*-07 *Topical Workshop on Electronic for Particle Physics*, Prague Czech Republic September 3–7 2007.

[18] K.N. Sjøbæk, *Full simulation of a testbeam experiment including modeling of the Bonn Atlas telescope and Atlas 3D pixel silicon sensors*, appendix C, M.Sc. thesis, Department of Physics, University of Oslo, Oslo Norway (2010) [INSPIRE].

2015 JINST 10 C06008